Supplementary Materials

"Resonant three-dimensional nonlinear sloshing in a square base basin. Part 5. Three-dimensional non-parametric tank forcing"

by O.M. Faltinsen, E.O. Lagodzinskyi, and A.N. Timokha

Appendix A. Details on the Narimanov-Moiseev–type modal equations

A.1. *Hydrodynamic coefficients*

Derivation details of the Narimanov-Moiseev–type modal system (2.6)–(2.8) are documented in Appendix A of the part 1. These are mainly devoted to how to compute the hydrodynamic coefficients starting with the so-called adaptive modal system. The derivations first introduce auxiliary tensors including $\Lambda^{(N-2)}_{\underbrace{i\dots m}_{N}}$ defined by the integrals

$$\Lambda^{(0)}_{ij}=\int_{-1/2}^{1/2} f^{(1)}_i f^{(1)}_j dx=\begin{cases}1, & i=j=0\\ 1/2, & i=j\neq 0,\\ 0, & i\neq j,\end{cases}$$

$$\Lambda^{(1)}_{i,j,k}=\int_{-1/2}^{1/2} f^{(1)}_i f^{(1)}_j f^{(1)}_k \mathrm{d}x=\frac{1}{2}\left(\Lambda^{(0)}_{|j-i|k}+\Lambda^{(0)}_{|i+j|k}\right),$$

.....

$$\Lambda^{(N-2)}_{\underbrace{i\dots m}_{N}}=\int_{-1/2}^{1/2}\underbrace{f^{(1)}_i\dots f^{(1)}_m}_{N}\mathrm{d}x=\frac{1}{2}\left(\Lambda^{(N-3)}_{|j-i|\dots m}+\Lambda^{(N-3)}_{|j+i|\dots m}\right)$$

and $\Lambda^{(-N)}_{mn,\underbrace{i\dots m}_{N}}$ is a family of tensors symmetric in nm and $i\dots m$, but comma means no symmetry between those groups of indexes. They are defined as

$$\Lambda^{(-0)}_{nm}=\int_{-1/2}^{1/2}(f^{(1)}_n)'(f^{(1)}_m)'\mathrm{d}x=\pi^2 nm\begin{cases}0, & nm=0,\\ 1/2, & n=m\neq 0,\\ 0, & n\neq m,\end{cases}$$

$$\Lambda^{(-1)}_{nm,i}=\int_{-1/2}^{1/2}(f^{(1)}_n)'(f^{(1)}_m)'f^{(1)}_i\mathrm{d}x=\pi^2 nm\frac{1}{2}\left(\Lambda^{(0)}_{|n-m|i}-\Lambda^{(0)}_{|n+m|i}\right),$$

.....

$$\Lambda^{(-N)}_{nm,\underbrace{i\dots k}_{N}}=\int_{-1/2}^{1/2}(f^{(1)}_n)'(f^{(1)}_m)'\underbrace{f^{(1)}_i\dots f^{(1)}_k}_{N}\mathrm{d}x=$$
$$\pi^2 nm\frac{1}{2}\left(\Lambda^{(N-1)}_{|n-m|\underbrace{i\dots k}_{N}}-\Lambda^{(N-1)}_{|n+m|\underbrace{i\dots k}_{N}}\right).$$

In these expressions, $f^{(1)}_n$ is defined in (2.3) and replacement $f^{(1)}_n(x)\to f^{(2)}_n(y)$, $\mathrm{d}x\to\mathrm{d}y$ will cause the same results for the square cross-section. In addition, we introduce the tensors, which depend on the non-dimensional liquid depth,

$$E_{n,k}=\lambda_{n,k}\tanh(\lambda_{n,k}h),\ D_{n,k}=\lambda^2_{n,k}/2,\ \lambda_{n,k}=\pi\sqrt{i^2+j^2}. \tag{A 1}$$

Derivations from the part 1 employ the auxiliary tensors:

$$
\begin{aligned}
&\Pi^{(0)}_{(n,k)(i,j)} = E_{n,k}\Lambda^{(0)}_{ni}\Lambda^{(0)}_{kj},\\
&\Pi^{(1)}_{(n,k)(i,j),(p,q)} = \Lambda^{(-1)}_{ni,p}\Lambda^{(1)}_{kjq} + r\Lambda^{(-1)}_{kj,q}\Lambda^{(1)}_{nip} + E_{n,k}E_{i,j}\Lambda^{(1)}_{nip}\Lambda^{(1)}_{kjq},\\
&\Pi^{(2)}_{(n,k)(i,j),(p,q)(a,b)} = \frac{1}{2}\left(\Lambda^{(-2)}_{ni,ap}\Lambda^{(2)}_{kj,bq} + \Lambda^{(-2)}_{kj,bq}\Lambda^{(2)}_{niap}\right)(E_{n,k} + E_{i,j}) +\\
&\qquad + \Lambda^{(2)}_{niap}\Lambda^{(2)}_{kjbq}(D_{n,k}E_{i,j} + D_{i,j}E_{n,k});
\end{aligned}
$$

$$
\begin{aligned}
&V^{1,(n,k)}_{(a,b)} = \frac{\delta_{an}\delta_{kb}}{E_{n,k}},\\
&V^{2,(n,k)}_{(a,b),(c,d)} = \left[E_{n,k}\Lambda^{(1)}_{nca}\Lambda^{(1)}_{kdb} - \frac{\Pi^{(1)}_{(n,k)(a,b),(c,d)}}{E_{a,b}}\right] \Big/ \left(E_{n,k}\Lambda^{(0)}_{nn}\Lambda^{(0)}_{kk}\right),\\
&V^{3,(n,k)}_{(a,b),(c,d),(e,f)} = \Bigg[D_{n,k}\Lambda^{(2)}_{ncea}\Lambda^{(2)}_{kdfb}\\
&- \frac{\Pi^{(2)}_{(n,k)(a,b),(c,d)(e,f)}}{E_{a,b}} - \Pi^{(1)}_{(n,k)(i,j),(e,f)}V^{2,(i,j)}_{(a,b),(c,d)}\Bigg] \Big/ \left(E_{n,k}\Lambda^{(0)}_{nn}\Lambda^{(0)}_{kk}\right),\\
&\bar{V}^{3,(n,k)}_{(a,b),(c,d)(e,f)} = \frac{1}{2}\left[V^{3,(n,k)}_{(a,b),(c,d),(e,f)} + V^{3,(n,k)}_{(a,b),(e,f),(c,d)}\right],
\end{aligned}
$$

where δ_{ij} is the Kronecker delta and, as usually, the repeated upper-lower indices mean summation (formally, infinite but, in reality finite due to specific properties of the above-introduced tensors). Using these tensors computes the following coefficients of the so-called adaptive multimodal system (Eqs. (2.15) in the part 1):

$$
\begin{aligned}
d^{1,(i,j)}_{(a,b),(c,d)} &= E^{i,j}V^{2,(i,j)}_{(a,b),(c,d)} + E_{i,j}\frac{\Lambda^{(1)}_{aci}\Lambda^{(1)}_{bdj}}{\Lambda^{(0)}_{ii}\Lambda^{(0)}_{jj}},\\
d^{2,(i,j)}_{(a,b),(c,d),(e,f)} &= E^{i,j}\bar{V}^{3,(i,j)}_{(a,b),(c,d)(e,f)} + \frac{E_{n,k}E_{i,j}\Lambda^{(1)}_{nei}\Lambda^{(1)}_{kfj}V^{2,(n,k)}_{(a,b),(c,d)}}{\Lambda^{(0)}_{ii}\Lambda^{(0)}_{jj}} + \frac{D_{a,b}E_{i,j}\Lambda^{(2)}_{acei}\Lambda^{(2)}_{bdfj}}{E_{a,b}\Lambda^{(0)}_{ii}\Lambda^{(0)}_{jj}},\\
t^{0,(i,j)}_{(a,b),(c,d)} &= E^{i,j}V^{2,(i,j)}_{(a,b),(c,d)} + \frac{rE_{i,j}\Pi^{(1)}_{(a,b)(c,d),(i,j)}}{2E_{a,b}E_{c,d}\Lambda^{(0)}_{ii}\Lambda^{(0)}_{jj}},\\
t^{1,(i,j)}_{(a,b),(c,d),(e,f)} &= 2E^{i,j}\bar{V}^{3,(i,j)}_{(a,b),(c,d)(e,f)} + \frac{E_{i,j}E_{n,k}\Lambda^{(1)}_{nei}\Lambda^{(1)}_{kfj}V^{2,(n,k)}_{(a,b),(c,d)}}{\Lambda^{(0)}_{ii}\Lambda^{(0)}_{jj}} + \frac{E_{i,j}\Pi^{(2)}_{(a,b)(c,d),(i,j)(e,f)}}{E_{a,b}E_{c,d}\Lambda^{(0)}_{ii}\Lambda^{(0)}_{jj}}\\
&\quad + \frac{E_{i,j}V^{2,(n,k)}_{(a,b),(e,f)}\Pi^{(1)}_{(n,k)(c,d),(i,j)}}{2E_{c,d}\Lambda^{(0)}_{ii}\Lambda^{(0)}_{jj}} + \frac{E_{i,j}V^{2,(n,k)}_{(c,d),(e,f)}\Pi^{(1)}_{(n,k)(a,b),(i,j)}}{2E_{a,b}\Lambda^{(0)}_{ii}\Lambda^{(0)}_{jj}}.
\end{aligned}
$$

The Narimanov-Moiseev–type modal system (2.6)–(2.8) is a particular case of the

adaptive system. It needs only finite subset of the tensors, i.e.,

$$d_1 = d^{1,(1,0)}_{(1,0),(2,0)} = t^{0,(1,0)}_{(1,0),(2,0)} + t^{0,(1,0)}_{(2,0),(1,0)},\quad d_2 = d^{2,(1,0)}_{(1,0),(1,0),(1,0)} = t^{1,(1,0)}_{(1,0),(1,0),(1,0)},$$
$$d_3 = d^{1,(1,0)}_{(2,0),(1,0)},\quad d_4 = d^{1,(2,0)}_{(1,0),(1,0)},\quad d_5 = t^{0,(2,0)}_{(1,0),(1,0)},\quad d_6 = d^{2,(1,0)}_{(1,0),(0,1),(0,1)},$$
$$d_7 = d^{1,(1,0)}_{(0,1),(1,1)} = t^{0,(1,0)}_{(0,1),(1,1)} + t^{0,(1,0)}_{(1,1),(0,1)},\quad d_8 = d^{2,(1,0)}_{(0,1),(0,1),(1,0)} + d^{2,(1,0)}_{(0,1),(1,0),(0,1)},$$
$$d_9 = d^{1,(1,0)}_{(1,1),(0,1)},\quad d_{10} = t^{1,(1,0)}_{(0,1),(0,1),(1,0)},\quad d_{11} = t^{1,(1,0)}_{(1,0),(0,1),(0,1)} + t^{1,(1,0)}_{(0,1),(1,0),(0,1)};$$
$$\hat{d}_1 = d^{1,(1,1)}_{(1,0),(0,1)} = d^{1,(1,1)}_{(0,1),(1,0)},\quad \hat{d}_3 = t^{0,(1,1)}_{(1,0),(0,1)} + t^{0,(1,1)}_{(0,1),(1,0)};$$
$$q_1 = d^{1,(3,0)}_{(1,0),(2,0)},\quad q_2 = d^{2,(3,0)}_{(1,0),(1,0),(1,0)},\quad q_3 = d^{1,(3,0)}_{(2,0),(1,0)},\quad q_4 = t^{1,(3,0)}_{(1,0),(1,0),(1,0)},$$
$$q_5 = t^{0,(3,0)}_{(1,0),(2,0)} + t^{0,(3,0)}_{(2,0),(1,0)},\quad q_6 = d^{1,(2,1)}_{(1,0),(1,1)},\quad q_7 = d^{2,(2,1)}_{(1,0),(1,0),(0,1)} + d^{2,(2,1)}_{(1,0),(0,1),(1,0)},$$
$$q_8 = d^{1,(2,1)}_{(0,1),(2,0)},\quad q_9 = d^{2,(2,1)}_{(0,1),(1,0),(1,0)},\quad q_{10} = d^{1,(2,1)}_{(2,0),(0,1)},\quad q_{11} = d^{1,(2,1)}_{(1,1),(1,0)},$$
$$q_{12} = t^{1,(2,1)}_{(1,0),(1,0),(0,1)},\quad q_{13} = t^{1,(2,1)}_{(1,0),(0,1),(1,0)} + t^{1,(2,1)}_{(0,1),(1,0),(1,0)},$$
$$q_{14} = t^{0,(2,1)}_{(1,0),(1,1)} + t^{0,(2,1)}_{(1,1),(1,0)},\ q_{15} = t^{0,(2,1)}_{(0,1),(2,0)} + t^{0,(2,1)}_{(2,0),(0,1)},$$

which determine the non-dimensional hydrodynamic coefficients at the nonlinear terms. The hydrodynamic coefficients at the linear terms are computed by (2.9) and (2.10), where g is the L-scaled gravity acceleration.

Coding the above-introduced computational formulas could be rather difficult. In order to get the quality control (or, alternatively, for engineering computations), we give the hydrodynamic coefficients listed in Tables 1–3.

A.2. *Linear damping rates*

The Narimanov-Moiseev–type modal equations (2.6)–(2.8) also contain the linear damping terms with the damping rates $\xi_{i,j}$. General assumption of the present and previous papers is that the rates accumulate an integral damping effect caused by diverse viscous phenomena, which keep the vortex components localised in relatively small subdomains so that, globally speaking, sloshing is satisfactory described within the framework of the modal theory that assumes an ideal liquid with irrotational flows. The linear damping in a clean tank is extensively discussed by Faltinsen & Timokha (2009, Chapter 6). In particular, the damping ratios $\xi_{i,j}$ are contributed by the linear boundary layer at the wetted tank surface. Faltinsen & Timokha (2009, Eq. (6.140)) gives the asymptotic approximation of the boundary-layer damping so that the corresponding damping rates are

$$\xi^{layer}_{i,j} = \sqrt{\frac{\nu}{2L^2\sigma_{i,j}}}\left[3 + 2\pi\frac{\sqrt{i^2+j^2}\,(0.5-h)}{\sinh(2\pi\sqrt{i^2+j^2}\,h)}\right] < \xi_{i,j} \qquad (\mathrm{A}\,2)$$

in terms of $\sqrt{\nu/(2L^2\sigma_{i,j})} \ll 1$, where ν is the kinematic viscosity coefficient. As discussed by Faltinsen & Timokha (2009, Sect. 6.3.1), (A 2) provides a rather accurate estimate of the damping ratios for the lower natural sloshing modes in a relatively large rectangular tank for the linear sloshing approximation. When $L \lesssim 0.2$ m, the experimental damping ratios may be larger than this theoretical value that can be explained by the dynamic contact angle (meniscus) effect. Faltinsen & Timokha (2009, Fig. 6.6) illustrated this fact by comparing the damping ratios for Lucite and glass basins , which are clearly different and larger than the estimate (A 2). The damping rates $\xi^{layer}_{i,j}$ tend to zero as the horizontal tank dimension L increases. However, this does not mean that the integral

TABLE 1. Hydrodynamic coefficients at the nonlinear terms in the modal equations (2.6), (2.7) versus the non-dimensional liquid depth.

h	d_1	d_2	d_3	d_4	d_5	d_6	d_7	d_8	d_9	d_{10}	d_{11}
0.42	3.1738	3.2851	-0.2256	-0.5153	-4.1403	-0.7109	1.3613	4.2239	0.1961	4.9348	-1.4218
0.44	3.1666	3.1756	-0.1987	-0.4473	-4.0114	-0.8142	1.3846	4.1206	0.2284	4.9348	-1.6283
0.46	3.1610	3.0822	-0.1751	-0.3890	-3.9002	-0.9017	1.4054	4.0331	0.2568	4.9348	-1.8033
0.48	3.1567	3.0021	-0.1543	-0.3388	-3.8041	-0.9761	1.4240	3.9587	0.2817	4.9348	-1.9522
0.50	3.1533	2.9333	-0.1360	-0.2955	-3.7209	-1.0396	1.4407	3.8952	0.3035	4.9348	-2.0792
0.52	3.1507	2.8739	-0.1199	-0.2581	-3.6486	-1.0940	1.4555	3.8408	0.3227	4.9348	-2.1879
0.54	3.1487	2.8226	-0.1057	-0.2256	-3.5857	-1.1406	1.4686	3.7942	0.3395	4.9348	-2.2812
0.56	3.1471	2.7781	-0.0932	-0.1974	-3.5310	-1.1807	1.4804	3.7541	0.3542	4.9348	-2.3615
0.58	3.1459	2.7394	-0.0822	-0.1729	-3.4832	-1.2153	1.4908	3.7195	0.3671	4.9348	-2.4306
0.60	3.1449	2.7058	-0.0725	-0.1516	-3.4415	-1.2452	1.5000	3.6896	0.3785	4.9348	-2.4903
0.62	3.1442	2.6765	-0.0639	-0.1330	-3.4050	-1.2710	1.5082	3.6638	0.3884	4.9348	-2.5420
0.64	3.1436	2.6509	-0.0563	-0.1167	-3.3731	-1.2933	1.5155	3.6415	0.3972	4.9348	-2.5867
0.66	3.1432	2.6285	-0.0497	-0.1025	-3.3451	-1.3127	1.5219	3.6221	0.4048	4.9348	-2.6255
0.68	3.1428	2.6090	-0.0438	-0.0901	-3.3205	-1.3296	1.5276	3.6052	0.4116	4.9348	-2.6591
0.70	3.1425	2.5918	-0.0386	-0.0792	-3.2990	-1.3442	1.5326	3.5906	0.4175	4.9348	-2.6884
0.72	3.1423	2.5768	-0.0341	-0.0696	-3.2801	-1.3569	1.5371	3.5779	0.4227	4.9348	-2.7139
0.74	3.1422	2.5636	-0.0301	-0.0613	-3.2635	-1.3680	1.5410	3.5668	0.4272	4.9348	-2.7361
0.76	3.1420	2.5521	-0.0265	-0.0539	-3.2490	-1.3777	1.5445	3.5571	0.4312	4.9348	-2.7554
0.78	3.1419	2.5419	-0.0234	-0.0474	-3.2361	-1.3861	1.5476	3.5487	0.4347	4.9348	-2.7723
0.80	3.1419	2.5330	-0.0206	-0.0418	-3.2249	-1.3935	1.5503	3.5413	0.4378	4.9348	-2.7870
0.82	3.1418	2.5252	-0.0182	-0.0368	-3.2149	-1.3999	1.5527	3.5349	0.4405	4.9348	-2.7998
0.84	3.1418	2.5183	-0.0160	-0.0324	-3.2062	-1.4055	1.5548	3.5293	0.4429	4.9348	-2.8111
0.86	3.1417	2.5122	-0.0141	-0.0285	-3.1985	-1.4104	1.5567	3.5244	0.4449	4.9348	-2.8209
0.88	3.1417	2.5069	-0.0125	-0.0251	-3.1918	-1.4147	1.5584	3.5201	0.4468	4.9348	-2.8295
0.90	3.1417	2.5022	-0.0110	-0.0221	-3.1858	-1.4185	1.5598	3.5163	0.4484	4.9348	-2.8370
0.92	3.1417	2.4981	-0.0097	-0.0195	-3.1806	-1.4218	1.5611	3.5130	0.4498	4.9348	-2.8436
0.94	3.1416	2.4944	-0.0086	-0.0172	-3.1759	-1.4247	1.5623	3.5101	0.4510	4.9348	-2.8493
0.96	3.1416	2.4912	-0.0075	-0.0152	-3.1719	-1.4272	1.5633	3.5076	0.4521	4.9348	-2.8544
0.98	3.1416	2.4884	-0.0067	-0.0134	-3.1683	-1.4294	1.5642	3.5054	0.4531	4.9348	-2.8588
1.00	3.1416	2.4859	-0.0059	-0.0118	-3.1651	-1.4313	1.5649	3.5035	0.4539	4.9348	-2.8627
1.10	3.1416	2.4773	-0.0031	-0.0063	-3.1541	-1.4380	1.5677	3.4968	0.4568	4.9348	-2.8760
1.20	3.1416	2.4727	-0.0017	-0.0033	-3.1483	-1.4415	1.5691	3.4933	0.4584	4.9348	-2.8830
1.30	3.1416	2.4702	-0.0009	-0.0018	-3.1452	-1.4433	1.5699	3.4915	0.4592	4.9348	-2.8866
1.40	3.1416	2.4689	-0.0005	-0.0010	-3.1435	-1.4443	1.5703	3.4905	0.4596	4.9348	-2.8886
1.50	3.1416	2.4682	-0.0003	-0.0005	-3.1426	-1.4448	1.5705	3.4900	0.4598	4.9348	-2.8896
1.60	3.1416	2.4678	-0.0001	-0.0003	-3.1421	-1.4451	1.5707	3.4897	0.4599	4.9348	-2.8901
1.70	3.1416	2.4676	-0.0001	-0.0001	-3.1419	-1.4452	1.5707	3.4896	0.4600	4.9348	-2.8904
1.80	3.1416	2.4675	-0.0000	-0.0001	-3.1417	-1.4453	1.5708	3.4895	0.4600	4.9348	-2.8906
1.90	3.1416	2.4675	-0.0000	-0.0000	-3.1417	-1.4453	1.5708	3.4895	0.4601	4.9348	-2.8906
2.00	3.1416	2.4674	-0.0000	-0.0000	-3.1416	-1.4453	1.5708	3.4895	0.4601	4.9348	-2.8907

damping rates $\xi_{i,j}$ seriously decreases for that limit, especially, for the resonant waves. A reason is that the resonant sloshing causes specific local free-surface phenomena including the wave breaking. Raynovskyy & Timokha (2018) discuss that for swirling in a circular base tank. The author experience with laboratory tank (see, also, the part 4) says that the actual value of $\xi_{0,1} = \xi_{1,0}$ should be, at least, two times larger than $\xi_{1,0}^{layer} = \xi_{0,1}^{layer}$ to fix the measured nonlinear resonant sloshing.

TABLE 2. Hydrodynamic coefficients at the nonlinear terms in the modal equations (2.7) and (2.8) versus the non-dimensional liquid depth.

h	$\hat{d}_1$	$\hat{d}_3$	q_1	q_2	q_3	q_4	q_5	q_6	q_7	q_8
0.42	0.6101	-3.0149	-0.7285	0.7541	-0.0518	12.8716	-10.9785	-0.1317	0.4863	3.3615
0.44	0.7042	-2.8599	-0.6361	0.6379	-0.0399	12.0783	-10.7720	-0.0661	0.1308	3.4318
0.46	0.7850	-2.7262	-0.5561	0.5422	-0.0308	11.4154	-10.5953	-0.0098	-0.1607	3.4917
0.48	0.8544	-2.6109	-0.4867	0.4629	-0.0238	10.8580	-10.4436	0.0388	-0.4014	3.5429
0.50	0.9142	-2.5112	-0.4264	0.3967	-0.0184	10.3866	-10.3129	0.0808	-0.6011	3.5870
0.52	0.9657	-2.4248	-0.3739	0.3411	-0.0142	9.9862	-10.2001	0.1172	-0.7676	3.6248
0.54	1.0101	-2.3500	-0.3281	0.2942	-0.0110	9.6444	-10.1024	0.1487	-0.9073	3.6576
0.56	1.0485	-2.2851	-0.2881	0.2544	-0.0085	9.3517	-10.0176	0.1762	-1.0249	3.6859
0.58	1.0816	-2.2287	-0.2532	0.2204	-0.0066	9.1001	-9.9440	0.2001	-1.1242	3.7105
0.60	1.1102	-2.1796	-0.2225	0.1915	-0.0051	8.8832	-9.8798	0.2210	-1.2085	3.7319
0.62	1.1351	-2.1369	-0.1957	0.1666	-0.0040	8.6957	-9.8239	0.2393	-1.2802	3.7505
0.64	1.1565	-2.0998	-0.1721	0.1452	-0.0031	8.5333	-9.7751	0.2552	-1.3413	3.7668
0.66	1.1752	-2.0674	-0.1515	0.1267	-0.0024	8.3923	-9.7324	0.2692	-1.3937	3.7809
0.68	1.1914	-2.0391	-0.1333	0.1107	-0.0019	8.2696	-9.6951	0.2815	-1.4386	3.7934
0.70	1.2054	-2.0144	-0.1174	0.0968	-0.0014	8.1627	-9.6624	0.2922	-1.4772	3.8042
0.72	1.2176	-1.9929	-0.1034	0.0848	-0.0011	8.0695	-9.6337	0.3016	-1.5105	3.8138
0.74	1.2282	-1.9740	-0.0910	0.0743	-0.0009	7.9880	-9.6086	0.3099	-1.5392	3.8221
0.76	1.2375	-1.9576	-0.0802	0.0651	-0.0007	7.9168	-9.5865	0.3172	-1.5639	3.8294
0.78	1.2455	-1.9432	-0.0706	0.0572	-0.0005	7.8544	-9.5671	0.3236	-1.5854	3.8359
0.80	1.2525	-1.9306	-0.0623	0.0502	-0.0004	7.7998	-9.5501	0.3292	-1.6040	3.8415
0.82	1.2586	-1.9195	-0.0549	0.0441	-0.0003	7.7519	-9.5351	0.3342	-1.6202	3.8465
0.84	1.2640	-1.9099	-0.0483	0.0388	-0.0002	7.7099	-9.5220	0.3385	-1.6342	3.8509
0.86	1.2686	-1.9014	-0.0426	0.0341	-0.0002	7.6730	-9.5104	0.3424	-1.6464	3.8547
0.88	1.2727	-1.8939	-0.0376	0.0300	-0.0001	7.6405	-9.5002	0.3457	-1.6570	3.8581
0.90	1.2762	-1.8874	-0.0331	0.0264	-0.0001	7.6120	-9.4912	0.3487	-1.6663	3.8611
0.92	1.2793	-1.8817	-0.0292	0.0232	-0.0001	7.5870	-9.4833	0.3513	-1.6744	3.8637
0.94	1.2820	-1.8767	-0.0257	0.0204	-0.0001	7.5650	-9.4764	0.3536	-1.6814	3.8660
0.96	1.2844	-1.8723	-0.0227	0.0180	-0.0001	7.5456	-9.4703	0.3557	-1.6876	3.8681
0.98	1.2865	-1.8684	-0.0200	0.0158	-0.0000	7.5285	-9.4649	0.3575	-1.6930	3.8699
1.00	1.2883	-1.8650	-0.0176	0.0140	-0.0000	7.5135	-9.4601	0.3591	-1.6977	3.8715
1.10	1.2945	-1.8533	-0.0094	0.0074	-0.0000	7.4614	-9.4436	0.3645	-1.7137	3.8770
1.20	1.2977	-1.8472	-0.0050	0.0039	-0.0000	7.4337	-9.4348	0.3675	-1.7220	3.8799
1.30	1.2994	-1.8440	-0.0027	0.0021	-0.0000	7.4190	-9.4301	0.3690	-1.7264	3.8814
1.40	1.3003	-1.8422	-0.0014	0.0011	-0.0000	7.4112	-9.4276	0.3699	-1.7287	3.8823
1.50	1.3008	-1.8413	-0.0008	0.0006	-0.0000	7.4070	-9.4263	0.3703	-1.7299	3.8827
1.60	1.3010	-1.8408	-0.0004	0.0003	-0.0000	7.4048	-9.4256	0.3705	-1.7305	3.8830
1.70	1.3011	-1.8406	-0.0002	0.0002	-0.0000	7.4036	-9.4252	0.3707	-1.7308	3.8831
1.80	1.3012	-1.8405	-0.0001	0.0001	-0.0000	7.4029	-9.4250	0.3707	-1.7310	3.8831
1.90	1.3012	-1.8404	-0.0001	0.0000	-0.0000	7.4026	-9.4249	0.3708	-1.7311	3.8832
2.00	1.3013	-1.8403	-0.0000	0.0000	-0.0000	7.4024	-9.4248	0.3708	-1.7311	3.8832

Appendix B. Steady-state periodic solutions

B.1. *Secular system*

The coefficients m_1, m_2 and m_3 in the secular system (3.2) are computed by the formulas

$$\begin{aligned} m_1 &= -\tfrac{1}{2}d_2 - d_1(p_0 - \tfrac{1}{2}h_0) - 2h_0 d_3, \\ m_2 &= -\tfrac{3}{4}d_6 + \tfrac{1}{4}d_{10} - \tfrac{3}{4}d_8 + \tfrac{1}{4}d_{11} - d_7 p_1 - h_1(\tfrac{1}{2}d_7 + 2d_9 - d_{12}), \\ m_3 &= -\tfrac{1}{4}d_6 + \tfrac{3}{4}d_{10} - \tfrac{1}{4}d_8 - \tfrac{1}{4}d_{11} - h_1(\tfrac{1}{2}d_7 + 2d_9 - d_{12}), \end{aligned} \tag{B 1}$$

TABLE 3. Hydrodynamic coefficients at the nonlinear terms in the modal equations (2.8) and coefficients m_1, m_2 and m_3 in the secular system (3.2) versus the non-dimensional liquid depth.

h	q_9	q_{10}	q_{11}	q_{12}	q_{13}	q_{14}	q_{15}	m_1	m_2	m_3
0.42	3.8728	0.6388	-0.0024	-1.3379	19.0706	-6.6174	-2.9862	-1.3957	-3.5038	3.2842
0.44	3.6611	0.6626	0.0294	-1.9260	17.8629	-6.4554	-2.9015	-1.5700	-3.5009	3.3511
0.46	3.4848	0.6808	0.0556	-2.4071	16.8568	-6.3174	-2.8304	-1.7109	-3.4967	3.4133
0.48	3.3372	0.6949	0.0770	-2.8032	16.0143	-6.1994	-2.7705	-1.8261	-3.4922	3.4705
0.50	3.2132	0.7056	0.0947	-3.1311	15.3053	-6.0982	-2.7197	-1.9210	-3.4878	3.5225
0.52	3.1086	0.7139	0.1093	-3.4041	14.7062	-6.0114	-2.6766	-1.9999	-3.4837	3.5695
0.54	3.0201	0.7203	0.1213	-3.6324	14.1980	-5.9367	-2.6398	-2.0659	-3.4801	3.6116
0.56	2.9450	0.7252	0.1312	-3.8242	13.7655	-5.8722	-2.6083	-2.1214	-3.4769	3.6493
0.58	2.8810	0.7290	0.1395	-3.9859	13.3962	-5.8166	-2.5813	-2.1684	-3.4743	3.6828
0.60	2.8264	0.7319	0.1463	-4.1229	13.0802	-5.7685	-2.5580	-2.2083	-3.4722	3.7126
0.62	2.7797	0.7341	0.1520	-4.2392	12.8090	-5.7269	-2.5379	-2.2425	-3.4705	3.7390
0.64	2.7397	0.7358	0.1567	-4.3382	12.5757	-5.6908	-2.5205	-2.2717	-3.4691	3.7623
0.66	2.7053	0.7372	0.1606	-4.4228	12.3748	-5.6595	-2.5054	-2.2969	-3.4681	3.7828
0.68	2.6757	0.7382	0.1639	-4.4953	12.2013	-5.6323	-2.4923	-2.3186	-3.4674	3.8010
0.70	2.6503	0.7390	0.1666	-4.5575	12.0513	-5.6086	-2.4809	-2.3374	-3.4668	3.8169
0.72	2.6283	0.7396	0.1688	-4.6110	11.9214	-5.5880	-2.4709	-2.3537	-3.4665	3.8310
0.74	2.6094	0.7401	0.1707	-4.6571	11.8087	-5.5701	-2.4622	-2.3678	-3.4662	3.8433
0.76	2.5930	0.7404	0.1723	-4.6969	11.7110	-5.5544	-2.4546	-2.3801	-3.4661	3.8542
0.78	2.5788	0.7407	0.1736	-4.7313	11.6260	-5.5408	-2.4480	-2.3909	-3.4661	3.8637
0.80	2.5665	0.7409	0.1747	-4.7610	11.5521	-5.5289	-2.4422	-2.4002	-3.4662	3.8721
0.82	2.5559	0.7411	0.1756	-4.7869	11.4877	-5.5185	-2.4371	-2.4084	-3.4663	3.8795
0.84	2.5466	0.7412	0.1764	-4.8093	11.4316	-5.5094	-2.4326	-2.4156	-3.4664	3.8859
0.86	2.5386	0.7413	0.1770	-4.8287	11.3827	-5.5015	-2.4287	-2.4219	-3.4666	3.8916
0.88	2.5316	0.7414	0.1775	-4.8457	11.3400	-5.4945	-2.4253	-2.4274	-3.4667	3.8966
0.90	2.5255	0.7414	0.1780	-4.8604	11.3027	-5.4884	-2.4222	-2.4322	-3.4669	3.9010
0.92	2.5202	0.7415	0.1784	-4.8733	11.2701	-5.4831	-2.4196	-2.4364	-3.4671	3.9048
0.94	2.5156	0.7415	0.1787	-4.8845	11.2416	-5.4785	-2.4172	-2.4401	-3.4673	3.9082
0.96	2.5116	0.7415	0.1789	-4.8942	11.2166	-5.4744	-2.4152	-2.4434	-3.4675	3.9111
0.98	2.5081	0.7416	0.1791	-4.9028	11.1948	-5.4708	-2.4134	-2.4463	-3.4677	3.9137
1.00	2.5051	0.7416	0.1793	-4.9102	11.1757	-5.4677	-2.4118	-2.4488	-3.4678	3.9160
1.10	2.4947	0.7416	0.1799	-4.9356	11.1103	-5.4569	-2.4062	-2.4575	-3.4685	3.9239
1.20	2.4894	0.7416	0.1801	-4.9488	11.0763	-5.4512	-2.4033	-2.4621	-3.4689	3.9280
1.30	2.4866	0.7416	0.1802	-4.9556	11.0585	-5.4483	-2.4017	-2.4646	-3.4692	3.9302
1.40	2.4852	0.7416	0.1802	-4.9592	11.0491	-5.4467	-2.4009	-2.4659	-3.4694	3.9313
1.50	2.4845	0.7416	0.1802	-4.9610	11.0442	-5.4459	-2.4005	-2.4666	-3.4695	3.9319
1.60	2.4841	0.7416	0.1802	-4.9620	11.0416	-5.4455	-2.4002	-2.4670	-3.4695	3.9323
1.70	2.4839	0.7416	0.1802	-4.9626	11.0402	-5.4453	-2.4001	-2.4672	-3.4695	3.9324
1.80	2.4837	0.7416	0.1802	-4.9628	11.0395	-5.4451	-2.4000	-2.4673	-3.4696	3.9325
1.90	2.4837	0.7416	0.1802	-4.9630	11.0391	-5.4451	-2.4000	-2.4673	-3.4696	3.9326
2.00	2.4837	0.7416	0.1802	-4.9631	11.0389	-5.4450	-2.4000	-2.4674	-3.4696	3.9326

where h_0, h_1 and p_0 appear in the asymptotic approximation of the second-order generlised coordinates

$$\begin{aligned} a_2 &= p_0(a^2+\bar{a}^2) + h_0(a^2-\bar{a}^2)\cos 2\sigma t + 2h_0 a\bar{a}\sin 2\sigma t + o(\epsilon),\\ b_2 &= p_0(\bar{b}^2+b^2) + h_0(\bar{b}^2-b^2)\cos 2\sigma t + 2h_0\bar{b}b\sin 2\sigma t + o(\epsilon),\\ c_1 &= p_1(a\bar{b}+\bar{a}b) + h_1(a\bar{b}-\bar{a}b)\cos 2\sigma t + h_1(\bar{a}\bar{b}+ab)\sin 2\sigma t + o(\epsilon); \end{aligned} \tag{B 2}$$

$$p_0 = \frac{d_4-d_5}{2\bar{\sigma}_{2,0}^2},\ h_0 = \frac{d_4+d_5}{2(\bar{\sigma}_{2,0}^2-4)},\ p_1 = \frac{2\hat{d}_1-\hat{d}_3}{2\bar{\sigma}_{1,1}^2},\ h_1 = \frac{2\hat{d}_1+\hat{d}_3}{2(\bar{\sigma}_{1,1}^2-4)}, \tag{B 3}$$

provided by the substitution $\sigma = \sigma_{1,0} = \sigma_{0,1}$ in (B 3) before these are used in (B 2). The coefficients m_1, m_2 and m_3 are listed in Table 3 versus h.

B.2. *Stability*

Faltinsen & Timokha (2017) employed the linear Lyapunov method and the multi-timing technique to study the stability of the steady-state sloshing associated with the amplitude parameters $a, \bar{a}, \bar{b}$ and b by (3.2). They introduced the slowly varying time $\tau = \frac{1}{2}\epsilon^{2/3}\bar{\sigma}t$, whose order is chosen according to the Moiseyev detuning $\bar{\sigma}^{-2} - 1 = O(\epsilon^{2/3})$, and express the perturbed solutions as

$$\begin{aligned} a_1 &= (a + \alpha(\tau))\cos\bar{\sigma}t + (\bar{a} + \bar{\alpha}(\tau))\sin\bar{\sigma}t + o(\epsilon^{1/3}), \\ b_1 &= (\bar{b} + \bar{\beta}(\tau))\cos\bar{\sigma}t + (b + \beta(\tau))\sin\bar{\sigma}t + o(\epsilon^{1/3}), \end{aligned} \tag{B 4}$$

where $a, \bar{a}, b$ and $\bar{b}$ come from (3.2). Inserting (B 4) into (2.6)–(2.8), gathering terms of the lowest asymptotic quantities order and keeping linear terms in $\alpha, \bar{\alpha}, \beta$ and $\bar{\beta}$ lead to the following linear system of ordinary differential equations

$$\mathbf{s}' + \xi\mathbf{s} + \mathcal{S}\,\mathbf{s} = 0, \tag{B 5}$$

where $\mathbf{s} = (\alpha, \bar{\alpha}, \beta, \bar{\beta})^T$, the prime is the differentiation by τ, and the matrix $\mathcal{S}$ has the following elements

$$\begin{aligned}
&s_{11} = -2m_1 a\bar{a} - (m_2 - m_3)b\bar{b}; \quad s_{12} = -\Lambda - m_1 a^2 - 3m_1\bar{a}^2 - m_2 b^2 - m_3\bar{b}^2, \\
&s_{13} = -2m_2\bar{a}b - (m_2 - m_3)a\bar{b}; \quad s_{14} = -2m_3\bar{a}\bar{b} - (m_2 - m_3)ab, \\
&s_{21} = \Lambda + 3m_1 a^2 + m_1\bar{a}^2 + m_2\bar{b}^2 + m_3 b^2; \quad s_{22} = 2m_1 a\bar{a} + (m_2 - m_3)b\bar{b}, \\
&s_{23} = 2m_3 ab + (m_2 - m_3)\bar{a}\bar{b}; \quad s_{24} = 2m_2 a\bar{b} + (m_2 - m_3)\bar{a}b, \\
&s_{31} = 2m_2 a\bar{b} + (m_2 - m_3)b\bar{a}; \quad s_{32} = 2m_3\bar{a}\bar{b} + (m_2 - m_3)ab, \\
&s_{33} = 2m_1 b\bar{b} + (m_2 - m_3)a\bar{a}; \quad s_{34} = \Lambda + m_1 b^2 + 3m_1\bar{b}^2 + m_2 a^2 + m_3\bar{a}^2, \\
&s_{41} = -2m_3 ab - (m_2 - m_3)\bar{a}\bar{b}; \quad s_{42} = -2m_2\bar{a}b - (m_2 - m_3)a\bar{b}, \\
&s_{43} = -\Lambda - 3m_1 b^2 - m_1\bar{b}^2 - m_2\bar{a}^2 - m_3 a^2; \quad s_{44} = -2m_1 b\bar{b} - (m_2 - m_3)a\bar{a}.
\end{aligned}$$

The fundamental solution $\mathbf{s} = \exp(\lambda\tau)\mathbf{a}$ of (B 5) follows from the spectral matrix problem $[(\lambda + \xi)E + S]\mathbf{a} = 0$, where λ are the unknown eigenvalues and $\mathbf{a}$ are the corresponding eigenvectors. Computations give the following characteristic bi-quadratic equation

$$(\lambda + \xi)^4 + s_1(\lambda + \xi)^2 + s_0 = 0, \tag{B 6}$$

where s_0 is the determinant of $\mathcal{S}$ and s_1 is a complicated function of the elements of $\mathcal{S}$. The eigenvalues λ can be expressed as $-\xi \pm \sqrt{x_{1,2}}$, where $x_{1,2} = \frac{1}{2}(-s_1 \pm \sqrt{s_1^2 - 4s_0})$ are two solutions of the quadratic equation $x^2 + s_1 x + s_0 = 0$. The fixed-point solution (associated with $a, \bar{a}, b$ and $\bar{b}$) is asymptotically stable ($\alpha, \bar{\alpha}, \beta$ and $\bar{\beta}$ exponentially decay with τ) if and only if the real component of λ is strongly negative.

The the stability condition can be written in as the alternative

$$\begin{aligned}
&\text{either} \quad s_1^2 - 4s_0 \geqslant 0 \;\&\; -s_1 + \sqrt{s_1^2 - 4c_s} \leqslant 0 \quad (\Leftrightarrow s_0 \geqslant 0 \;\&\; s_1 \geqslant 0)\,, \\
&\text{or} \quad s_1^2 - 4s_0 \geqslant 0 \;\&\; -s_1 + \sqrt{s_1^2 - 4s_0} > 0 \;\&\; \sqrt{\tfrac{1}{2}\left(-s_1 + \sqrt{s_1^2 - 4s_0}\right)} < \xi, \\
&\text{or} \quad s_1^2 - 4s_0 < 0 \;\&\; \sqrt{2\sqrt{s_0} - s_1} < \xi.
\end{aligned} \tag{B 7}$$

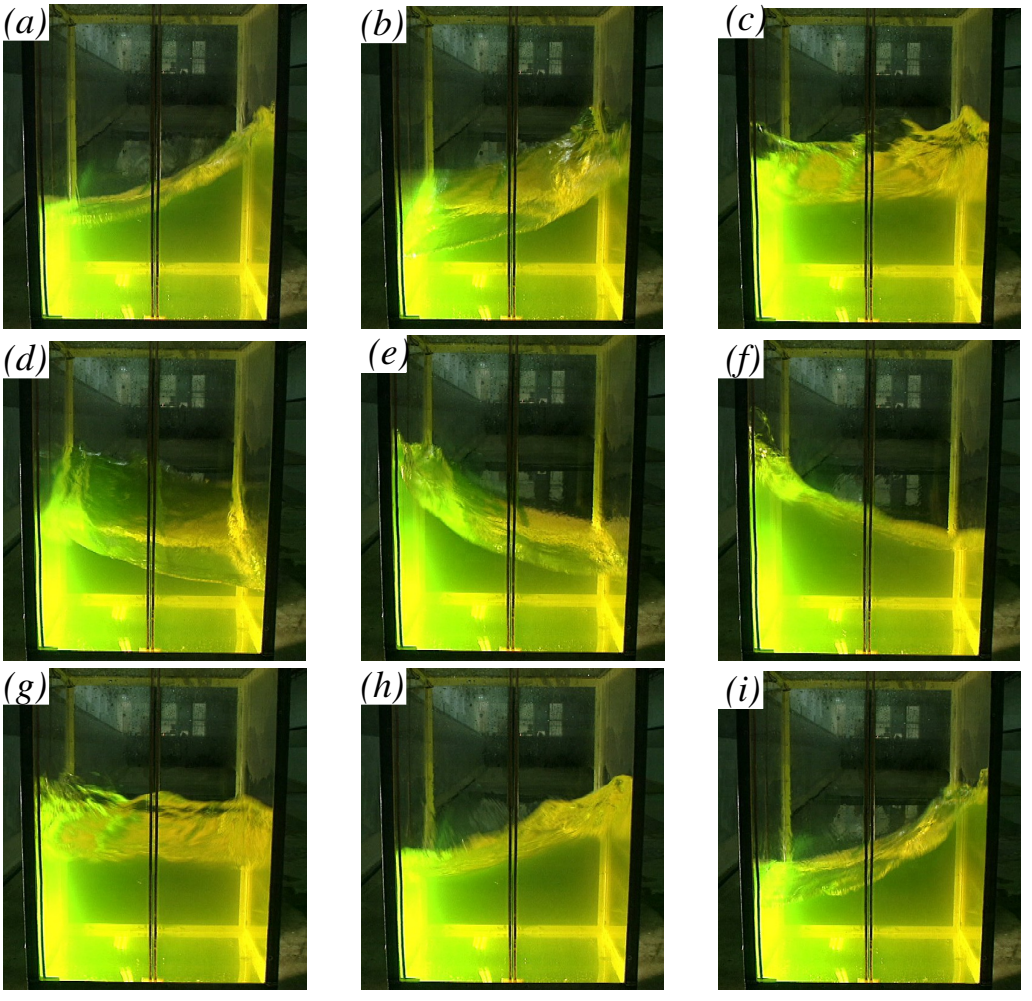

FIGURE 1. Snap shoots (from (a) to (i), the part 1) demonstrating the counterclockwise (top view) swirling in a square base tank for the non-dimensional liquid depth $h = 0.508$ and the longitudinal forcing with $\eta_{1a} = 0.0078$. The excitation frequency is equal to the lowest natural frequency.

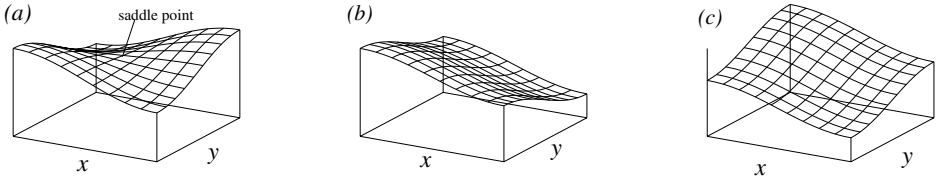

FIGURE 2. Sketches of three-dimensional wave patterns associated with the natural sloshing mode $[f_1^{(1)}(x) f_1^{(2)}(y)]$ (panel a) as well as the diagonal combined Stokes modes (panels b and c). The panels are taken from the part 1.

B.3. *Visualisation of the steady-state wave modes*

Figure 3 classifies the steady-state wave modes introducing of swirling, (nearly-) standing (planar, diagonal and squares-like) types and 'irregular' steady-state waves. Based on the experimental observations and measurements, the part 1 and Ikeda *et al.* (2012) discuss the wave modes and even publishes some photos. Swirling is best illustrated in figure 1, which is taken from the part 1. The figure shows both swirling phenomena and associated wave breaking, which, as we discussed above, causes an extra damping in the hydrodynamic system.

The lowest-order approximation of the planar wave mode is simply associated with the Stokes waves by (2.3) but the diagonal and squares-like waves are mainly contributed by the combined Stokes modes $S(x, y; \alpha, \beta)$, which was introduced in (3.31). The part 1 discusses these waves as well as the combined Stokes modes by depicting the diagonal wave profiles. The latter is represented in figure 2.

Appendix C. The longitudinal harmonic forcing

When $\delta_1 = 0$, (3.18) leads to the equations

$$B[\Lambda + m_1 B^2 + (m_3 - F)A^2] = 0 \text{ and } \; B[DA^2 - \xi] = 0, \tag{C 1}$$

whose solutions are either $B = 0$ (the planar standing wave occurring in the excitation plane Oxz) or $B \neq 0$ (the swirling wave mode). The planar standing wave is governed by

$$A^2 \left[(\Lambda + m_1 A^2)^2 + \xi^2\right] = \epsilon^2, \;\; B = 0 \tag{C 2}$$

but the amplitude parameters for swirling follow from the system

$$\begin{cases} A^2 \left[(\Lambda + m_1 A^2 + (m_3 - F)B^2)^2 + (D\,B^2 + \xi)^2\right] = \epsilon^2, \\ \Lambda + m_1 B^2 + (m_3 - F)A^2 = 0, \\ DA^2 - \xi = 0. \end{cases} \tag{C 3}$$

Taking A^2 from the last equation, substituting it into the second one, and, finally, inserting the obtained expressions for A^2 and B^2 into the first equation, leads, as Faltinsen & Timokha (2017) showed, to the algebraic equation with respect to $C > 0$ (because $D > 0$):

$$q_6 C^6 + q_5 C^5 + q_4 C^4 + q_3 C^3 + q_2 C^2 + q_1 C + q_0 = 0, \tag{C 4}$$

where

$$\begin{aligned}
q_6 &= \xi^3 (m_1^2 - m_3^2)^2 > 0, \\
q_5 &= 2\xi^2 \Lambda\, (m_3 - m_2)(m_3 + m_1)(m_1 - m_3)^2, \\
q_4 &= \xi \left[\xi^2 [3m_1^4 + (m_2^2 - 6m_2 m_3 - m_3^2)m_1^2 - 2m_1 m_3 (m_2 - m_3)^2 + m_2 m_3^2 (m_2 + 2m_3)] \right. \\
&\quad \left. + \Lambda^2 (m_2 - m_3)^2 (m_1 - m_3)^2 \right], \\
q_3 &= \epsilon^2 (m_2 - m_3)^3 m_1^2 + 2\Lambda\xi^2 \left[m_1 (m_2^3 - m_2^2 m_3 + m_2 m_3^2 - m_3^3) \right. \\
&\quad \left. + (m_2 - m_3)(m_1^2 (m_2 + m_3 - 2m_1) - m_2 m_3 (m_2 + m_3)) \right], \\
q_2 &= \xi \left[\Lambda^2 (m_2 - m_3)^2 (m_1 - m_2)^2 \right. \\
&\quad \left. + \xi^2 [3m_1^4 + (-m_2^2 - 6m_2 m_3 + m_3^2)m_1^2 - 2m_1 m_2 (m_2 - m_3)^2 + m_2^2 m_3 (2m_2 + m_3)] \right], \\
q_1 &= 2\xi^2 \Lambda\, (m_3 - m_2)(m_1 + m_2)(m_1 - m_2)^2, \\
q_0 &= \xi^3 (m_1^2 - m_2^2)^2 > 0
\end{aligned}$$

are functions of the forcing frequency parameter Λ. Equation (C 4) has maximum six positive roots. Substituting these roots in expressions for A^2 and B^2 computes $(\sigma/\sigma_1, A, B)$, which implies a point on the corresponding response curves.

REFERENCES

Faltinsen, O. M. & Timokha, A. N. 2009 *Sloshing*. Cambridge: Cambridge University Press.

Faltinsen, O. M. & Timokha, A. N. 2017 Resonant three-dimensional nonlinear sloshing in a square-base basin. Part 4. Oblique forcing and linear viscous damping. *Journal of Fluid Mechanics* **822**, 139–169.

Ikeda, T., Ibrahim, R. A., Harata, Y. & Kuriyama, T. 2012 Nonlinear liquid sloshing in a square tank subjected to obliquely horizontal excitation. *Journal of Fluid Mechanics* **700**, 304–328.

Raynovskyy, I. & Timokha, A. 2018 Damped steady-state resonant sloshing in a circular base container. *Fluid Dynamics Research* **50**, Article ID 045502.